

# Ion beam processing of metal surfaces for improved corrosion resistance \*

E. McCafferty, P.M. Natishan and G.K. Hubler

Naval Research Laboratory, Washington, DC 20375, USA

Ion beam techniques such as ion implantation, ion beam mixing, and ion beam assisted deposition allow modification of metal surfaces for improved corrosion resistance. The corrosion process can be altered by modifying either the anodic or cathodic process, by modifying the passive film, or by using corrosion resistant coatings. Examples are given of each approach. These are, in turn, implantation of various ions into aluminum to improve the resistance to pitting, ion implantation or ion beam mixing of palladium into titanium to increase the corrosion resistance in acids, implantation to form amorphous surface alloys, and the use of ion beam deposition to form protective films of tantalum oxide or silicon nitride on aluminum.

## 1. Introduction

The ability to modify metal surfaces with ion beams has afforded the corrosion scientist a new flexibility in attempting to improve the corrosion resistance of metals. At the Naval Research Laboratory, for example, there has been an extensive program aimed at improving corrosion resistance using the techniques of ion implantation, ion beam mixing, and ion beam assisted deposition (IBAD), as well as laser surface alloying and processing [1].

It is well known that aqueous corrosion proceeds through the operation of microscopic coupled anodic and cathodic processes. Thus, ion beam surface modification can be utilized so as to interfere with the corrosion process by: 1) modification of the anodic process, or 2) modification of the cathodic process. Other approaches involve: 3) improvement of the passive film, and 4) use of corrosion-resistant coatings.

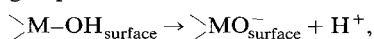
Examples of each of these four approaches will be given from research performed at or in collaboration with the Naval Research Laboratory. Earlier papers should also be consulted in some cases for more detail [2–6].

## 2. Modification of the anodic process

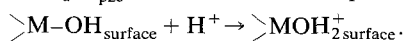
The first step in the pitting corrosion of passive metals in chloride solutions is adsorption of the chloride ion on the oxide-covered surface. Subsequent steps involve penetration or dissolution through the oxide film,

followed by local reaction of the underlying metal with the environment. The exact mechanism of pitting corrosion is not yet known in great detail, and various mechanisms have been proposed [7], but it is clear that the first step in the breakdown process involves the adsorption of  $\text{Cl}^-$  ions.

Ion implantation offers a means for altering the acid-base character of oxide films so as to alter the adsorption of  $\text{Cl}^-$  ions and accordingly the pitting behavior. It is widely appreciated that the outermost layer of oxide surfaces and of oxide-covered metal surfaces consists of hydroxyl groups [8]. These hydroxyl groups remain undissociated in aqueous solutions at a pH specific to the oxide in question and called the pH of zero charge,  $\text{pH}_{\text{pzc}}$  [2]. Thus, at the pH of zero charge, the oxide surface has no net charge. For aqueous solutions of higher pH, the oxide surface has a negative charge due to the dissociation of hydroxyl groups:



whereas in aqueous solutions where the pH is lower than  $\text{pH}_{\text{pzc}}$ , the oxide surface is positively charged:



It is these latter type of surfaces to which  $\text{Cl}^-$  ions are attracted so as to initiate the pitting process.

The pH of zero charge, and thus the surface charge character, is a function of the individual cation M contained in the M–OH bond. Fig. 1 illustrates in a schematic manner the surface charge character in the range of pH 0–14 and the  $\text{pH}_{\text{pzc}}$  of several oxides. As seen in the diagram, at a solution pH of 7, the surface of aluminum oxide (and of oxide-covered aluminum) consists of acidic groups (positively charged) onto which  $\text{Cl}^-$  ions will adsorb. Aluminum, in fact, is susceptible

\* Supported by the Office of Naval Research, Arlington, Virginia, USA, under the guidance of A.J. Sedriks.

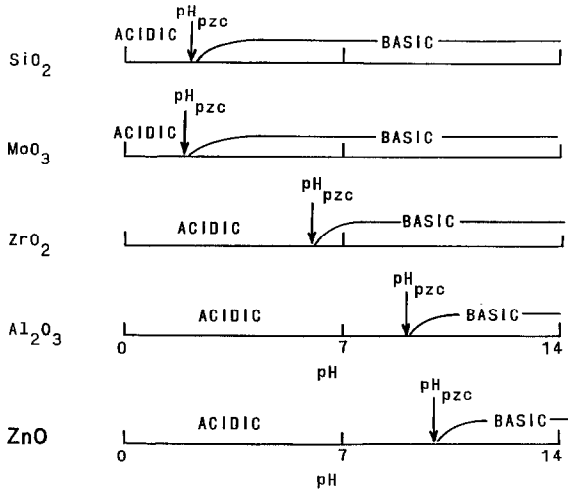


Fig. 1. Surface charge character of various oxides between pH 0 and 14 in relation to the pH of zero charge,  $pH_{pzc}$ .

to pitting attack. Fig. 2 shows that aluminum is passive up to its pitting potential, i.e. the electrode potential at which there is an abrupt increase in the anodic current density due to the initiation of corrosion pits.

Using fig. 1 as a guide, we have implanted into aluminum metals such as Zr, Mo, Si, and Ta (all with oxides having a  $pH_{pzc}$  lower than that of  $Al_2O_3$ ) and have observed an increase in the pitting potential, i.e. in the susceptibility to pitting attack. Conversely, implantation with Zn (for which zinc oxide has a higher  $pH_{pzc}$  than that of  $Al_2O_3$ ) decreases the pitting potential. The results for the various implanted ions are summarized in fig. 3. There is some scatter in the correlation between the pH of zero charge of the oxide and the pitting potential of the oxide-covered metal due to the fact that different systems displayed differing resultant surface concentrations of the implanted ion in the oxide film.

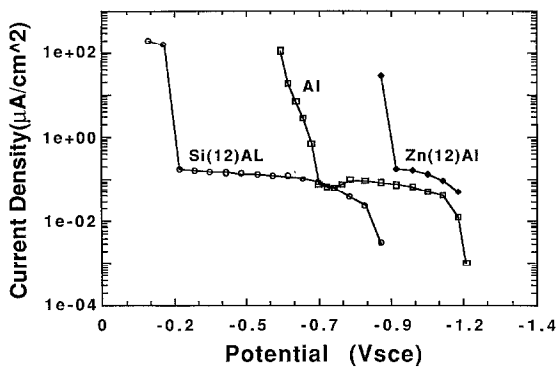


Fig. 2. Anodic polarization curves for aluminum, Si-implanted aluminum, and Zn-implanted aluminum in de-aerated 0.1M NaCl. (The direction of anodic polarization, as in figs. 4 and 6, is from right to left).

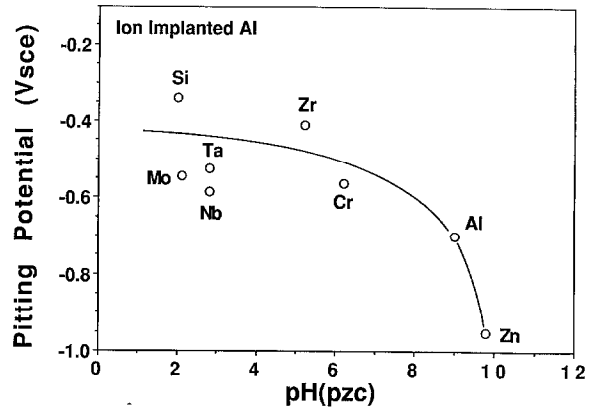


Fig. 3. Effect of various implanted ions on the pitting potential of aluminum in de-aerated 0.1M NaCl.

However, each of the implanted ions selected because their oxide has a lower pH of zero charge than that of  $Al_2O_3$  leads to an improved resistance to pitting, in accord with our pH of zero charge model. These results for ion-implanted surface alloys have been confirmed in two different laboratories for thicker binary alloys produced by sputter deposition techniques [9,10].

### 3. Modification of the cathodic process

This type of modification often involves alloying of a noble metal into a more active metal which normally undergoes an active-passive transition in the electrolyte of interest. The basic idea is illustrated in the experimental results shown in fig. 4 for titanium with and without surface-alloyed palladium. Titanium alone undergoes spontaneous active corrosion in the electrolyte (1M  $H_2SO_4$  at  $100^\circ C$ ) with the anodic polarization curve for titanium dissolution (shown in fig. 4) and the cathodic polarization curve for hydrogen evolution (not

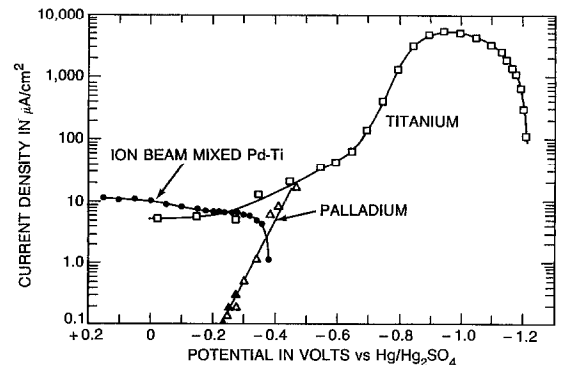


Fig. 4. Anodic polarization curves for titanium and Pd-implanted titanium and the cathodic polarization curve for palladium in  $H_2SO_4$  at  $100^\circ C$ .

shown in the figure) intersecting at the naturally occurring open circuit corrosion potential of  $-1.2$  V vs  $\text{Hg}/\text{Hg}_2\text{SO}_4$ . The corrosion rate in this freely corroding state is  $3700 \mu\text{A}/\text{cm}^2$ . As seen in fig. 4, titanium can be passivated by anodic polarization, but the electrode is driven through very high anodic current densities and suffers extensive surface damage enroute to the passive region.

When titanium is surface alloyed with palladium, either by ion implantation or by ion beam mixing, the role of surface Pd atoms is to provide sites for the cathodic reaction so that hydrogen evolution occurs predominantly on Pd (at a higher rate than on Ti at any given potential). The resulting mixed potential is more positive than the critical potential for passivation of titanium; and the open circuit potential for the surface alloy lies in the passive region of titanium, rather than in the active state, as for unalloyed titanium.

Fig. 4 shows in fact that the cathodic polarization curve for hydrogen evolution on pure Pd intersects the anodic polarization curve for pure Ti in the passive region of Ti at an electrode potential of ca.  $-0.45$  V, which would be the naturally occurring corrosion potential for an alloy containing equal fractional areas of Pd and Ti. Fig. 4 shows that the open circuit corrosion potential of the ion beam mixed surface alloy is ca.  $-0.40$  V, and the surface alloy self passivates with a corresponding corrosion rate of  $10 \mu\text{A}/\text{cm}^2$ , or about a 400-fold decrease in the corrosion rate of unalloyed titanium.

#### 4. Improvement of the passive film

In recent years it has been shown that the aqueous corrosion resistance of certain amorphous alloys is greater than that of the corresponding crystalline alloys [11]. This observation has triggered a number of studies involving ion implantation with metalloid ions, such as P, B, or C, to produce amorphous surface alloys. Two representative examples of this approach will be cited here.

Clayton, Wang and Hubler [5] have implanted P, B, and P + B into 304 and 316 stainless steels and have produced amorphous surface alloys. Implantation of P into 304 or 316 stainless steel reduced the critical current density for passivation in  $0.5\text{M H}_2\text{SO}_4$  or in  $0.5\text{M H}_2\text{SO}_4 + 0.5\text{M NaCl}$  whereas B implantation had no effect on the passivation of either stainless steel. However, P implantation had no effect on the pitting potential in the chloride electrolyte whereas B implantation raised the pitting potential.

Hubler, McCafferty and coworkers [6] implanted Ti at high fluences into 52100 steel to produce an amorphous surface. The amorphous layer was formed only at high fluences when sputter erosion of the surface

caused implanted Ti atoms to emerge. The gettering of hydrocarbons in the ambient vacuum by the surface Ti atoms caused appreciable inward diffusion of C, which in turn stabilized an amorphous Fe-Ti-C layer. The amorphous surface layer provided modest improvement in corrosion resistance in  $1\text{N H}_2\text{SO}_4$  and in  $0.1\text{N NaCl}$  but localized attack at inclusion eventually led to undermining of the amorphous layer at high anodic overvoltages.

#### 5. Use of corrosion-resistant coatings

This approach in effect substitutes a more corrosion-resistant material for the substrate, which is retained for other desirable properties, such as low cost or high strength. One of the most promising of the ion beam surface techniques is ion beam assisted deposition (IBAD) of coatings. IBAD is a relatively new technique involving concurrent physical vapor deposition and ion implantation to produce a modified surface region thicker than that resulting from ion implantation alone and having greater adhesion than physical vapor deposited coatings. Another attraction of the IBAD technique is that it allows some imagination in choosing interesting combinations of coatings and substrates.

Fig. 5 is a schematic diagram of the apparatus used to produce IBAD coatings. The sample is positioned in

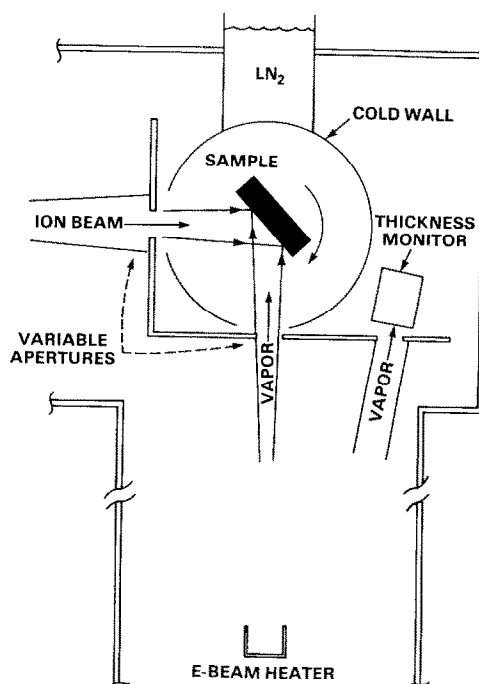


Fig. 5. Apparatus for ion beam assisted deposition (IBAD) of coatings.

Table 1  
Ion beam assisted deposited coatings on aluminum

Chemical species	Thickness [ $\mu\text{m}$ ]	Ion beam energy [eV]	$E_{\text{pit}}$ [V vs SCE]	$\Delta E_{\text{pit}}^{\text{a}}$ [V]
$\text{Ta}_2\text{O}_5$	0.5	None	-0.300	+0.400
	0.5	250 $\text{O}_2^+$	-0.350	+0.350
	0.5	500 $\text{O}_2^+$	+0.300	+1.000
$\text{Si}_3\text{N}_4$	0.01	500 $\text{N}_2^+$ (89%)	-0.400	+0.300
		$\text{N}^+$ (11%)		
	0.2	500 $\text{N}_2^+$ (89%)	0.000	+0.700
		$\text{N}^+$ (11%)		
	2.0	500 $\text{N}_2^+$ (89%)	0.050	+0.750
		$\text{N}^+$ (11%)		

<sup>a</sup> Compared to pure aluminum.

the center of a chamber 30 cm above an electron beam evaporator and can be rotated so that the surface is exposed simultaneously to the evaporant from below and an ion beam from the side. The thickness of the deposited material and the rate of deposition (generally between 1 and 8  $\text{\AA}/\text{s}$ ) is measured with a quartz crystal oscillator and rate monitor. Concurrently with the deposition, an ion beam of selected ionic species is directed onto the substrate. Variable apertures are used to limit the deposition and ion bombardment to specific areas on the substrate. Ion energies typically range from 0.1 to 40 keV and fluxes range from  $1 \times 10^{14}$  to  $1 \times 10^{15}$  ions  $\text{cm}^{-2} \text{s}^{-1}$ . A liquid-nitrogen-cooled cold wall surrounds the substrate to trap contaminate gases. The chamber is equipped with a precision leak valve that will direct a flow of gas directly onto the substrate. The base pressure of the chamber is  $5 \times 10^{-7}$  Torr, and the reactive gases are introduced into the chamber to pressures ranging from  $1 \times 10^{-5}$  to  $5 \times 10^{-5}$  Torr.

In preliminary work [1], we have shown that 0.2 micron thick  $\text{Cr}_2\text{O}_3$  IBAD coatings on 52100 steel provided partial protection in dilute chloride and in sulfuric

acid solutions. The results of more recent work involving tantalum oxide or silicon nitride IBAD coatings on aluminum in 0.1M NaCl are summarized in table 1, and several polarization curves are shown in fig. 6. As seen in table 1, either  $\text{Ta}_2\text{O}_5$  or  $\text{Si}_3\text{N}_4$  coatings on aluminum increase the resistance to pitting attack. The effectiveness of the coating depends on the processing conditions. For 0.5 micron  $\text{Ta}_2\text{O}_5$  coatings, the coating exposed to the 250 eV beam of  $\text{O}_2^+$  ions displayed the same pitting potential as the vapor deposited coating (although each of these two samples were effective in raising the pitting potential by about 400 mV). The IBAD sample processed at 500 eV, however, provided an additional 600 mV increase in  $E_{\text{pit}}$ , or an increase of 1000 mV above the pitting potential of uncoated aluminum. For the  $\text{Si}_3\text{N}_4$  IBAD coatings which were all processed at the same ion energy and ion flux, the pitting potential increases with the thickness of the coating.

## 6. Summary

Several research examples been given to illustrate that ion beam surface modification techniques can be used to control corrosion processes, and that systems of interest can be selected by application of the principles of corrosion science.

## References

- [1] E. McCafferty, G.K. Hubler, P.M. Natishan, P.G. Moore, R.A. Kant and B.D. Sartwell, Mater. Sci. Eng. 86 (1987) 1.
- [2] P.M. Natishan, E. McCafferty and G.K. Hubler, J. Electrochem. Soc. 135 (1988) 321.
- [3] E. McCafferty, P.M. Natishan and G.K. Hubler, Corros. Sci. 30 (1990) 209.

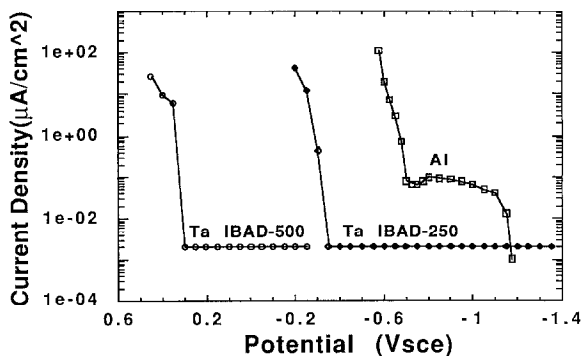


Fig. 6. Anodic polarization curves for aluminum and for 0.5  $\mu\text{m}$  thick tantalum oxide films on aluminum prepared by ion beam assisted deposition at 250 and 500 eV.

- [4] E. McCafferty and G.K. Hubler, *J. Electrochem. Soc.* 125 (1978) 1892.
- [5] C.R. Clayton, Y.-F. Wang and G.K. Hubler, in: *Passivity of Metals and Semiconductors*, ed. M. Froment (Elsevier, Amsterdam, 1983) p. 305.
- [6] G.K. Hubler, P.P. Trzaskoma, E. McCafferty and I.L. Singer, in: *Ion Implantation into Metals*, eds. V. Ashworth, W.A. Grant and R.P.M. Proctor (Pergamon, Oxford, 1982) p. 24.
- [7] Z. Szklarska-Smialowska, *Pitting Corrosion of Metals* (National Association of Corrosion Engineers, Houston, 1986).
- [8] See, for example: J.C. Bolger, in: *Adhesion Aspects of Polymeric Coatings*, ed. K.L. Mittal (Plenum, New York, 1983) p. 3.
- [9] G.D. Davis, W.C. Moshier, T.L. Fitz and G.O. Cote, *J. Electrochem. Soc.* 137 (1990) 422.
- [10] G.S. Frankel, M.A. Russak, C.V. Jahnes, M. Mirzamaani and V.A. Brusic, *J. Electrochem. Soc.* 136 (1989) 1243.
- [11] K. Hashimoto, in: *Passivity of Metals and Semiconductors*, ed. M. Froment (Elsevier, Amsterdam, 1983) p. 235.